

Efficient Communication Acceleration for Next-Gen Scale-up Deep Learning Training Platforms

Saeed Rashidi*, Srinivas Sridharan§, Sudarshan Srinivasan†, Matthew Denton* and Tushar Krishna*

*Georgia Institute of Technology, Atlanta, USA

§Facebook, Menlo Park, USA

†Intel, Bangalore, India

saeed.rashidi@gatech.edu, ssrinivas@fb.com, sudarshan.srinivasan@intel.com,
matthewdenton@gatech.edu, tushar@ece.gatech.edu

ABSTRACT

Deep Learning (DL) training platforms are built by interconnecting multiple DL accelerators (e.g., GPU/TPU) via fast, customized interconnects. As the size of DL models and the compute efficiency of the accelerators has continued to increase, there has also been a corresponding steady increase in the bandwidth of these interconnects.

Systems today provide 100s of gigabytes (GBs) of interconnect bandwidth via a mix of solutions such as Multi-Chip packaging modules (MCM) and proprietary interconnects (e.g., NVlink) that together form the scale-up network of accelerators. However, as we identify in this work, a significant portion of this bandwidth goes under-utilized. This is because (i) using compute cores for executing collective operations such as all-reduce decreases overall compute efficiency, and (ii) there is memory bandwidth contention between the accesses for arithmetic operations vs those for collectives, and (iii) there are significant internal bus congestions that increase the latency of communication operations.

To address this challenge, we propose a novel microarchitecture, called *Accelerator Collectives Engine* (ACE), for DL collective communication offload. ACE is an extension to the conventional Network Interface (NIC) tuned to cope with the high-bandwidth and low latency requirements of scale-up networks and is able to efficiently drive the various scale-up network systems (e.g. switch-based or point-to-point topologies). We evaluate the benefits of the ACE with micro-benchmarks (e.g. single collective performance) and popular DL models using an end-to-end DL training simulator. ACE significantly accelerates the average raw latency of collective communication operations observed in DL training workloads such as all-reduce and all-to-all by $1.53\times$ and $1.21\times$, respectively. For modern DL workloads, ACE on average increases the network bandwidth utilization by $1.97\times$, resulting in $2.71\times$ and $1.44\times$ speedup in iteration time for ResNet-50 and GNMT, respectively.

1. INTRODUCTION

Deep Learning (DL) and Deep Neural network (DNN) models are being deployed pervasively across a wide range

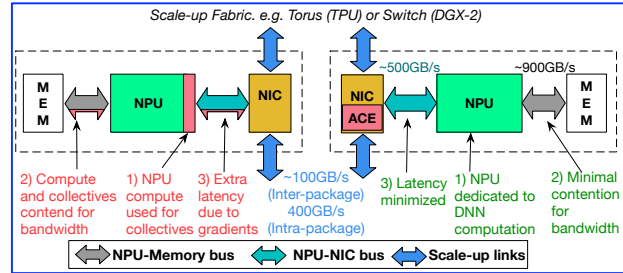


Figure 1: Baseline system vs. ACE

of real-world application domains such as image classification, natural language processing, and autonomous driving. The size and computational requirements of these DNN models are growing at an unparalleled rate, $2\times$ every 3.4 months [5], to handle the unrelenting growth in data and workload requirements. The advent of energy-efficient inference accelerators capable of handling these large models and need for accelerating training time when dealing with 10s to 100s of petabytes of input data is raising the demand for faster and more efficient DL training solutions.

Today's DL training platforms are built by interconnecting multiple accelerators (e.g., GPUs, TPUs, FPGAs), henceforth called *Neural Processing Units* (NPUs) in the interest of generality, together through different network fabrics, running distributed DL training algorithms. This is because a single accelerator cannot satisfy the compute, memory, and I/O requirements of today's state-of-the-art DNNs. Distributed DL training fundamentally involves splitting the DNN model, training data, or both across multiple NPUs. These schemes are referred to as model, data, and hybrid parallel respectively.

The parallelization strategy in turn dictates the communication required between NPUs. This communication is "collective" in nature, i.e., all NPUs synchronize input/output/error activations during the forward/backward pass, and gradients during the backward pass. Specifically, two collective operations: all-to-all and all-reduce, occur heavily during distributed DL training. These operations are often latency-sensitive (since the next layer of the DNN cannot proceed un-

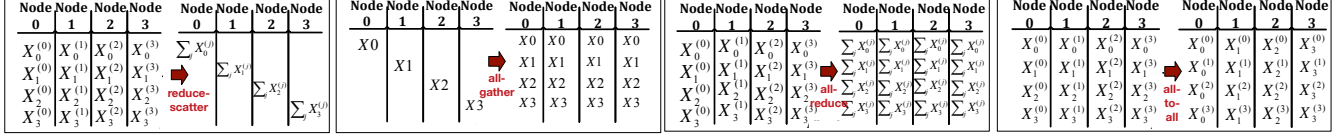


Figure 2: Overview of collective communication operations used in DNN training networks.

til gradients have been synchronized¹) and bandwidth hungry due to the large sizes of the activations/gradients and limited network bandwidth and hence can easily become bottleneck [30, 42]. There has thus been extensive work on optimizing DL training communication on current platforms; spanning algorithms [28, 15], frameworks [21, 4, 23], communication libraries [22, 8, 35], and high-bandwidth interconnects [29].

This work identifies a key challenge with the current mechanisms by which collective communication is orchestrated, and shows that this would become worse in future systems. Specifically, we focus on *scale-up* networks that connect accelerators within one or more chassis directly, through interconnect fabric, and do not require CPU host involvement in the communication data-path.²

Fig. 1 shows a NPU and its connected peripherals. We identify three sources of inefficiency. (i) **Compute**: a portion of the compute resources of the NPU are used for performing collective updates and driving the network, which reduces the compute available to training computations (e.g., GEMMs during the forward and backward passes), (ii) **Memory Bandwidth**: the received gradients need to be written to and read from memory, in turn reducing the bandwidth available for the actual training computations which is known to be highly bandwidth-intensive in modern DNNs, and (iii) **Communication Latency**: communicating the gradients over the NPU-NIC and NPU-MEM buses adds latency overhead. To the best of our knowledge, this is the first work to identify these issues in both modern systems (via real experiments on NVIDIA DGX-1 and Intel Xeon Skylake) and future systems (modeled in a detailed simulator). The implication of these three issues is under-utilization of the available scale-up bandwidth as systems scale.

To address these challenges, we propose *Accelerator Collectives Engine (ACE)*, which is a microarchitecture support for NIC designed to handle distributed DL training collective operations and cope with the high bandwidth demand of scale-up network. With ACE, (i) NPU resources are totally free to perform training algorithms only, (ii) the memory bandwidth is freely available for training computation only, and (iii) the NPU-MEM and NPU-NIC buses are significantly less congested and are used only for initial and final data-transfer to/from ACE on-chip memory. This is shown in Fig. 1.

Previous works have demonstrated the efficiency of collective offload to either smart NICs or network switches for the scale-out network that involves host CPU intervention [46, 20, 16, 30, 42, 32, 25]. However, these CPU-initiated schemes require explicit resource reservations that will be exacerbated

¹We assume synchronous updates which provide better guarantees at convergence than asynchronous updates

²In contrast, the *scale-out network*, i.e. the network connecting host CPUs together through Ethernet or other network fabrics, require accelerators to rely on the host for both control/datapath. Hence, scale-out is used to connect individual scale-up networks. This will be explored as part of future work.

for shared memory systems as the number of network packets grows, eventually limiting the scalability. ACE is a smart NIC-based system for accelerator-based systems and can be integrated in different system topologies such as switch based or point-to-point (e.g. Torus) systems, contrasting our work against switch offload proposals that limit their usability to only switch based networks. We contrast ACE against prior works in Table 1.

This paper makes the following contributions:

- We identify a set of key challenges in the end-points of DL training platforms related to compute, memory bandwidth and communication latency that can limit the utilization of available scale-up network bandwidth for future training platforms.
- We propose a novel offload engine, called *Accelerator Collectives Engine (ACE)*, designed to tuned to handle collective communication and efficiently drive scale-up network utilization.
- ACE achieves $1.53 \times$ speedup for all-reduce and $1.21 \times$ for all-to-all collective operations (in terms of raw communication latency). For modern DL workloads such as ResNet-50 [19] and GNMT [48], ACE gets $2.71 \times$ and $1.44 \times$ better performance (on average) in iteration time over the state-of-the-art bandwidth-equivalent baselines, respectively. ACE improves network bandwidth utilization by $1.97 \times$ compared to baseline systems.

The rest of the paper is organized as follows: Section 2 presents the necessary background for distributed training systems. Section 3 establishes the challenges in scaling DL training, specifically focused on critical bottlenecks in the endpoint that inhibit efficient network utilization. Section 4 describes the ACE microarchitecture. This is followed by a detailed description of our evaluation and simulation methodology in Section 5 and the experimental results in Section 6. Next, we compare our work against related work in Section 7. Finally, we conclude the paper in Section 8.

2. BACKGROUND

Training DNNs involves iteratively refining the parameters (aka weights) of the network by solving a non-convex, non-linear optimization problem to minimize a loss function. Here, we provide background on distributed training [37, 11].

Parallelization. The most common parallelization technique for speeding up DL training is called *data parallelism*. It replicates the entire model on multiple nodes to take advantage of the large number of input samples. Every node computes partially trained weight gradients for its subset of samples of the input data, aka mini-batch. At the end of each iteration, nodes exchange their partially trained weight gradients and perform the SGD operation to update the weights gradients accumulated from all nodes. The updated weights, are then used in the forward pass of the next iteration. In *model*

Table 1: Comparison of previous SmartNIC and switch offload schemes against ACE.

Scheme	Workload	Compute	Offload	Protocol	Topology	Aggregation
Mellanox [3]	HPC, DL	CPU or Accel	Switch	Infiniband	Switch-based	Collective
Barefoot [1]	DL	CPU or Accel	Switch	Ethernet	Switch-based	Collective
sPIN [20]	HPC	CPU	NIC	Ethernet	Switch-based	Collective
Triggered [46]	HPC	CPU	NIC	RDMA-based	Flexible	Collective
Inceptionn [31]	DL	Accel	NIC	Ethernet	Tree	Parameter Server
NVIDIA [13]	DL	Accel (GPU)	Switch	Shared Memory	Switch-based	Collective (All-Reduce only)
ACE	DL	Accel	NIC	RDMA-based	Flexible	Collective

Table 2: Communication payloads for different parallelism approaches.
FP:Forward Pass. BP: Back Pass

Parallelism	Activations (FP)	Weight grad (BP)	Input grad (BP)
Data		✓	
Model	✓		✓
Hybrid	partially	partially	partially

Table 3: ResNet-50 communication time and NW utilization

Number cores	1	2	4	8	16
Time (ms)	89.8	45.1	22.2	18.4	18.0
Utilization (%)	17%	34%	70%	84%	86%

parallelism, all nodes have the same datasets and work on the same mini-batch, but the model is divided among nodes. Each node thus produces a part of the output activations and input gradients during the forward pass and back-propagation, respectively, and these values must be communicated across all nodes to enable forward pass and back-propagation for all nodes. Table 2 describes the data being exchanged for various parallelism approaches.

Collective Communication Operations. Exchanges of input/weight gradients and output activations among the nodes, depending on the parallelism approach, is known as "collective communication". In general, four different collective communication operations are the main contributor in DNN training communication, as shown in Fig. 2: (i) reduce-scatter, (ii) all-gather, (iii) all-reduce, and (iv) all-to-all. Reduce-scatter reduces (e.g. sum) all data, initially residing in the nodes, such that at the end each node has a portion globally reduced data. All-gather gathers the data, initially scattered across nodes, such that at the end all of nodes have all of the data. All-reduce can be thought of a reduce-scatter followed by an all-gather. In all-to-all, each node needs to send different portion of data to other nodes. All-reduce is the dominant communication pattern observed in the DL training for exchanging gradients and activations in various parallelism schemes. However, all-to-all is used in some scenarios such as table embedding exchanges for recommendation models [34].

Topology-Aware Collective Algorithm. Collectives have efficient implementations algorithm based on the underlying topology. Libraries like NVIDIA NCCL [35] provide different implementations for collectives, such as ring-based, tree-based, hierarchical, direct all-reduce/all-to-all, to optimize for the available bandwidth in the underlying topology [45, 7, 38]. We will discuss this further in Section 5, where we consider topology-aware collectives for evaluating our target systems.

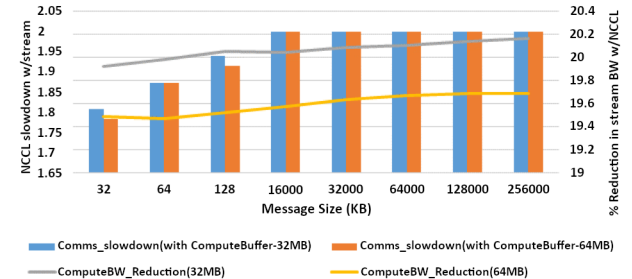


Figure 3: Impact of Memory Bandwidth on NVIDIA NCCL Allreduce.

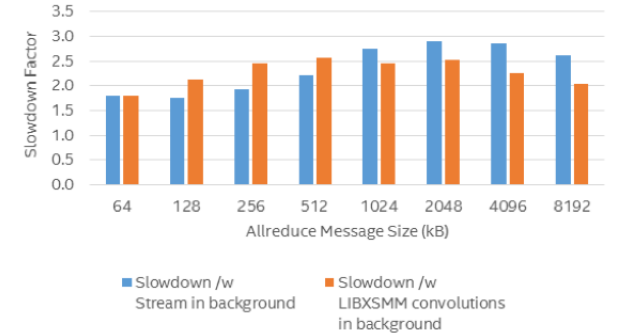


Figure 4: Impact of Memory Bandwidth on Intel MLSL Allreduce.

3. MOTIVATION: POOR SCALE-UP BANDWIDTH UTILIZATION

In this section, we identify some critical challenges in scaling DL training, both on current and future platforms. Fig. 1 qualitatively summarizes our findings.

NPU Compute Availability. On modern systems, a fraction of NPU cores (e.g. CUDA cores) *asynchronously* execute/orchestrate DL training collective communication operations while the majority of compute cores execute DL computation (e.g. GEMMs and Convolutions). Collective operations, such as allreduce, are parallelized across these cores since a single NPU core cannot fully saturate memory bandwidth and network bandwidth given various bottlenecks in the NPU core - memory - network data-path [22, 35]. Each core iterates over a sequence of send/receive operations to/from peers followed by an optional computation on data that was received with locally available data (e.g. reduction sum). Therefore, the optimal number of NPU cores is a function of network bandwidth saturated by a single core, memory bandwidth available to a single core, communication algorithm, message size, and so on. Table Table 3 presents the number of CPU cores and the effective network bandwidth utilization when running ResNet-50 allreduce message sizes

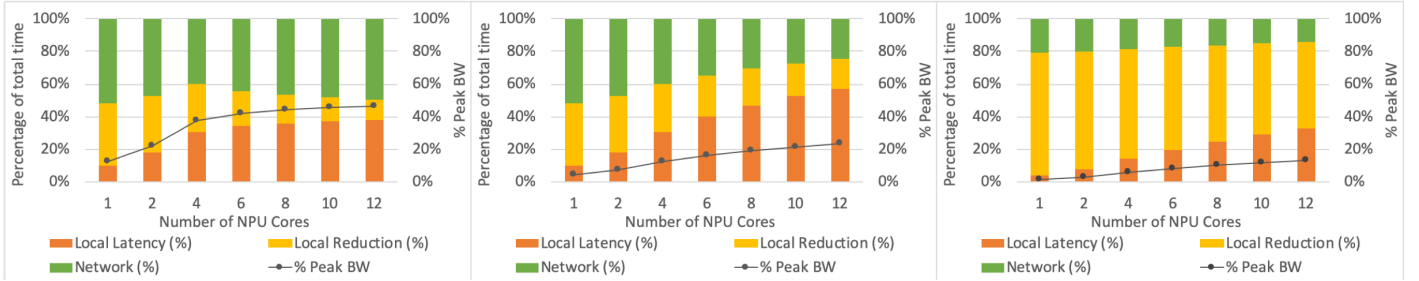


Figure 5: Time breakdown for an all-reduce on a 2D Torus topology for (a) baseline, (b) NW optimized: baseline with 3x network bandwidth, (c) Memory bandwidth contention: NW optimized with 20% read memory bandwidth per NPU core.

on 32-nodes with dual-socket Intel Xeon Skylake processors and 100G Intel Omnipath fabric. Given significant latency overheads in executing collective communication operations, even on latency-optimized Intel Xeon CPUs, we observe we need 4-8 cores to efficiently drive the network - cores that would otherwise be used in executing DL computation.

Memory Bandwidth Contention. Fig. 3 presents the negative impact or slowdown of allreduce collective when run concurrently with the *Stream benchmark* [2] (mimicking memory bandwidth hungry DL compute) on NVIDIA and Intel platforms. On a NVIDIA DGX-1 system, we observed an average 2 \times slowdown for NCCL allreduce³ when run concurrently with the Stream benchmark over an unloaded system running only NCCL allreduce. The two bars represents the slowdown of NCCL allreduce for messages from 32KB to 256MB when running with either 32MB or 64MB Stream buffer sizes. Additionally, we observed a 19% drop in the achieved Steam memory bandwidth when run concurrently with the NCCL allreduce benchmark compared to only running the Stream benchmark. A 20% drop in memory bandwidth will have a drastic impact on compute time since most DL compute kernels are memory bound. Similarly, on Intel Xeon Skylake processors we observed 2-3 \times slowdown for MLSL allreduce [22] when run concurrently with the Stream benchmark or LIBXsmm convolution kernels running ResNet-50 [19] operations.

Scale-Up Bandwidth Utilization. We developed a simple analytical model to highlight some of these issues. The analytical model captures time spent in the performing local reduction sum (streaming operation involving two local memory reads, sum operation, and local write), remote network write (e.g. RDMA write and synchronization), and various other per-NPU local latency overheads (e.g. scheduling, processing message headers etc.) incurred in each step of an allreduce collective. We assume a 2D-torus topology with 16 NPUs arranged in 4x4 grid. Each NPU (1GHz, 1TB/s memory bandwidth) has 4 links, with each link at 25GB/s uni-directional bandwidth and 95% link efficiency. We assume each NPU core can read 64 bytes/clock and write 32 bytes/clock, resulting in 64GB/s and 32GB/s of read and write bandwidth respectively. We assume the reduction sum operation and local write are completely overlapped by the local reads and other overheads. In an ideal case, we need 4 NPUs (2 bytes of local load for each byte of remote write)

³We expect to observe similar behavior on DGX-2 as well. The impact would be higher in general given DGX-2's NVSwitch is more efficient than DGX-1 Hybrid Cubic Mesh

to achieve sufficient memory bandwidth to match network bandwidth (100GB/s). Fig. 5 presents the time breakdown and % peak bandwidth achieved with 1 to 12 NPU cores used to parallelize a single 16MB allreduce for three scenarios: (a) 2us latency for each step in the allreduce (very aggressive for any modern NPU architecture), (b) 3x network bandwidth, (c) 3x network bandwidth with 20% read memory bandwidth (12.8GB/s) per NPU. We generally observe the bandwidth utilization to drop from 50% to 15% we go from Fig. 5(a)-(c). due to increased latency and reduction overheads. In other words, we believe addressing endpoint overheads must be prioritized over adding more network bandwidth.

Overall, we observe the challenge of using NPU cores, i.e. GPU CUDA cores or CPU cores, for executing collective communication - the increased contention to memory bandwidth for performing the local reduction sum operation and various other scheduling overheads negatively affects collective performance across different architectures. In other words, the complex interplay among compute-memory-network not only affects collective performance but also the performance of compute kernels executing concurrently. This in turn increases the effective compute time available for overlapping asynchronous communication operations - hiding deep inefficiencies in how systems are designed. These challenges are expected to get exacerbated in future training platforms, where better compute accelerators and/or hierarchical bandwidths due to emerging MCM technologies [10] will make it harder to hide communication behind compute.

4. ACCELERATOR COLLECTIVES ENGINE

We propose a novel micro-architecture for DL collective communication offload called ACE. Fig. 6 shows the high-level overview of ACE integrated into the NIC module. Upon activation, ACE loads initial data to be communicated into its SRAM (from NPU main memory) via NIC TX DMA. The incoming/outgoing traffic is stored into NIC SRAM temporally. ACE receives incoming scale-up network gradients/activations through NIC SRAM, and directly stores and processes them, requiring no further communication with NPU. ACE also writes back data to NIC SRAM for sending data to other nodes. Finally, ACE transfers the results to the NPU main memory through NIC RX DMA. This decoupling method enables conventional NIC components to focus on handling communication protocol (e.g. packetizing, depacketizing) while allowing ACE to focus on processing and executing the collective operation. Also, it allows ACE to be bypassed and NIC falls back to normal operation mode when needed.

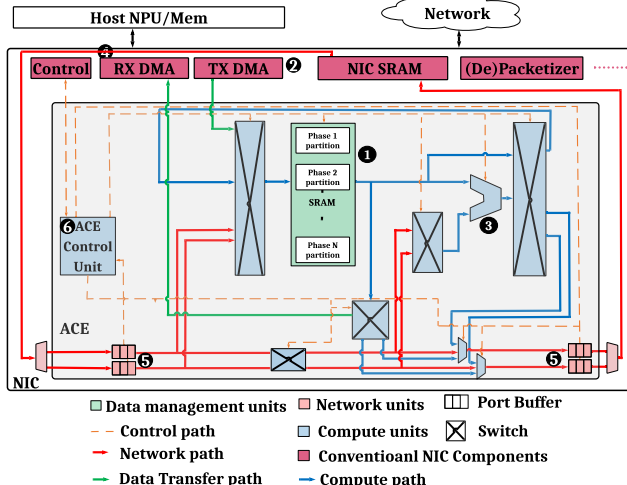


Figure 6: ACE microarchitecture. #1 is the on-chip SRAM. #2 is the NIC TX DMA for transferring data from main memory to NIC SRAM (normal operation) or ACE SRAM (ACE activated). #3 is the ALU. #4 is the NIC RX DMA for transferring data from NIC SRAM (normal operation mode) or ACE SRAM (ACE activated mode) to main memory. #5 are the input/output port buffers. These buffers are allocated per each physical link and contain packets corresponding for that specific link. #6 is the control unit logic.

This section describes the details of operation, and the features within ACE that make it flexible across various network topologies and collective algorithms.

Table 4: Data granularity at different levels of ACE execution.

Granularity	Size	Constraint
Payload (variable)	Training Algorithm	Training Algorithm
Chunk (64kB on avg.)	Parameter for Pipelining	Storage Element Size (Area/Power)
Message (4kB on avg.)	Parameter - Multiple of Number of Nodes	Topology
Packet (256B)	Link Technology	Technology
Flit (256B)	Network Buffer Size	Microarchitecture (Area/Power)
Phit (variable)	Link Width	Technology

4.1 Data Granularity

Table 4 shows the granularity of data at different levels of the ACE execution and their determining factor. It also shows the default value of each level used in ACE. ACE initiates execution by receiving a command from NPU to perform a specific collective on a *payload*. The payload could be activations or gradients depending on the parallelism approach and forward/back pass (Table 2). The command includes the collective type and the address range for data residing in the main memory. ACE then divides the payload into multiple chunks and begins processing and scheduling of each chunk individually and in a pipelined manner.

A chunk itself decomposes into multiple messages and the collective algorithm runs at message granularity. The number of messages is a multiple of the number of nodes in the system. For e.g., if the ACE wants to perform an all-reduce in a ring with 4 NPUs, it can divide the chunk into 8 messages, and execute all-reduce serially over two steps⁴. Multiple chunks can however be scheduled to run in parallel. The degree of parallelism for running the chunks depends

⁴Each step leads to processing & performing all-reduce for a group of 4 messages and the algorithm is ring-based. More details on ring-based all-reduce is provided in Section 4.2

on the number of state machines within the ACE control unit (details in Section 4.3.2) to handle the dataflow for each chunk. Each message comprises of one or more packets when it enters the network layer. The unit of data processing within the ACE is packets. The bus width and SRAM interface might or might not be equal to the size of the packets and data movement/execution is serialized if the size is smaller than packet width. Each packet is split into multiple flits and each flit consists of multiple phits (depending on the link speed) as it traverses the physical link.

4.2 Walk-Through Example for All-Reduce

We describe ACE in action via a detailed walk-through example for running the ring-based all-reduce collective over a ring for both the baseline and ACE vs. system as shown in Fig. 7a. The general concepts and the main advantages of ACE compared to the baseline are applicable to any topology/collective, as we describe later in Section 4.5.

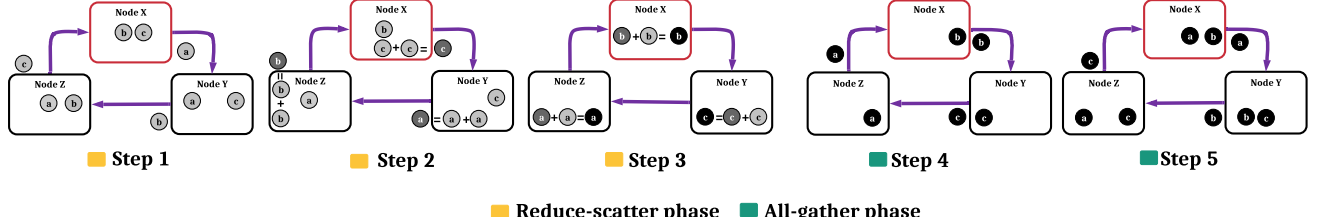
Fig. 7a(a) shows the logical flow of the algorithm across the different nodes. We assume one chunk for simplicity. Since there are three nodes, there are three messages⁵. An all-reduce can be implemented as a reduce-scatter followed by an all-gather, as can be seen from Fig. 2. Steps 1-3 are the reduce-scatter phase. Step 1 initiates the reduce-scatter; each node simply sends one message to its neighbor and waits for receiving another message from its other neighbor. In step 2, each node reduces the received message with its local message and forwards to the next. Step 3 concludes the reduce-scatter by each node reducing the last message it has received. All-gather starts by each node forwarding a copy of its reduced message to its neighbor (step 4) and then each node keeping a copy of its received message and forwarding it to its neighbor (steps 5 and 6).

Fig. 7b shows this flow from node X's view in the case of baseline vs. ACE. It is clear from this figure that in baseline, in all phases, messages need to go all the way from/to main memory to/from NIC to be injected/received into/from network. The local reduction is done through a series of back and forth data movements between NPU and main memory resulting in congestion on both NPU-Mem and NPU-NIC busses. This in turn reduces the available memory bandwidth and compute power for the training algorithm. In contrast, ACE restricts the data movement only to the first and last phases (reduced congestion and increased available memory bandwidth) and allows the training algorithm to make use of complete NPU compute power.

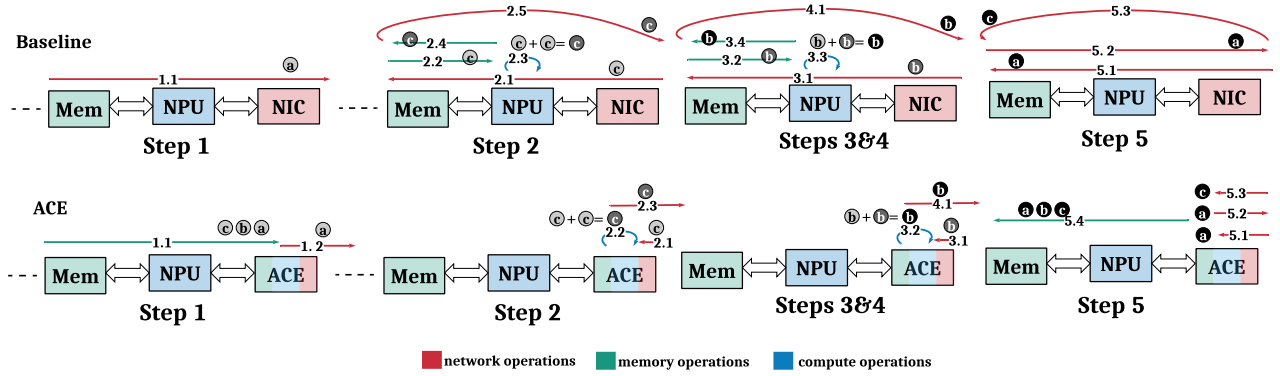
Fig. 7c shows the internal ACE interactions for node X. Here, the ACE SRAM is divided into two partitions - one serves as a source for the (only one) all-reduce phase, and the last one serves as the source to hold the final results to send back to main memory. In step 1, the three messages are brought into the first partition of ACE SRAM by the TX DMA (sub-step 1.1). Then, one message is sent out through a series of packets⁶ injected into the designated output port buffer to be written to NIC SRAM (sub-step 1.2). In step 2,

⁵Note that there could be multiple number of 3 messages and as we described in Section 4.1, they should be executed in serial. But here for simplicity we assume only 1 group of 3 messages.

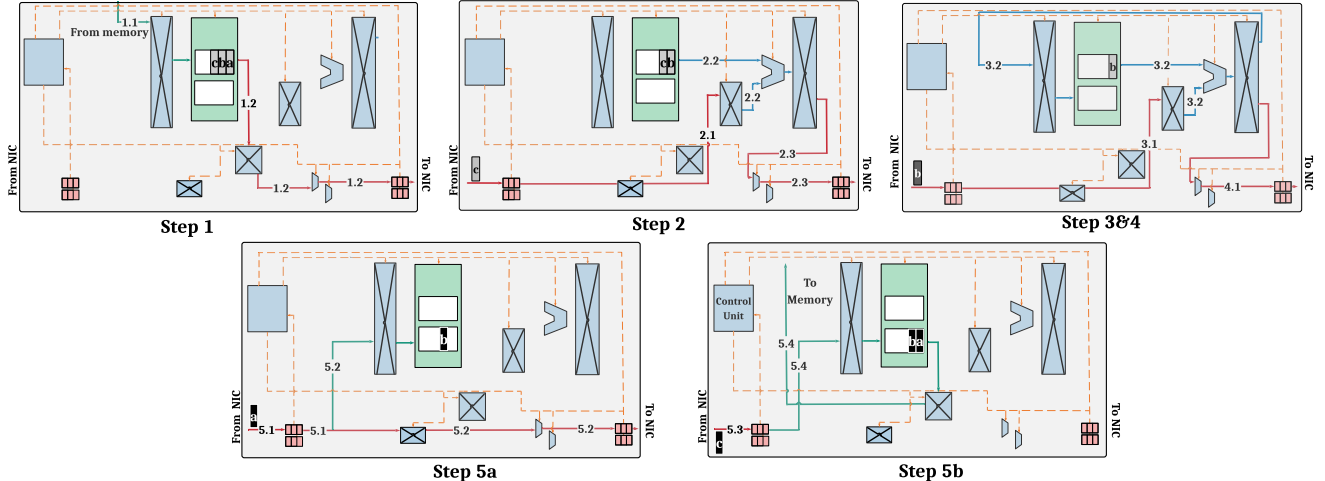
⁶Note that here packets means packet data. The actual packetization of this data is the job of NIC once it wants to send it over the links.



(a) Indication of all-reduce on a ring.



(b) Flow of compute/mem/network operations for ring all-reduce in the baseline vs. ACE from the viewpoint of node X



(c) Steps of ring all-reduce within ACE microarchitecture for node X

Figure 7: Steps showing the comparison between baseline vs. ACE for single ring all-reduce.

the received message is reduced with the local data (sub-step 2.2) and is forwarded to the neighbor (sub-step 2.3). ACE overlaps steps 3 and 4 of the algorithm; after performing a reduction (sub-step 3.2), stores it locally (sub-step 3.2) and forwards to the next neighbor (sub-step 4.1) at the same time. Step 5 is broken into two figures for more clarity. In step 5a, the received message is stored and forwarded (sub-step 5.2) at the same time, while in step 5b, the final received message is stored and the whole chunk is sent back to the main memory by RX DMA (sub-step 5.4).

It is clear that in some steps within ACE, multiple resources should be available for some sub-steps to proceed. For example, in sub-step 5.2 in step 5a, both the SRAM input port

should be available and the output port should have the free space. In such cases, if any of the resources are not free, that step is stalled until all resources are available. Multiple chunks can be executed in parallel to maximize internal hardware resources and link bandwidth, as we discuss more in Section 4.3.2.

4.3 Parallelism

In order to achieve high network utilization, we need to apply parallelism at various levels. From the algorithmic perspective, there are several levels where parallelism is possible. Assuming the collective algorithm has P phases, multiple chunks can run in parallel both within a phase and across

different phases. Each chunk will send/receive multiple messages. Hence, multiple in-flight chunks mean multiple in-flight messages (belonging to different chunks) are possible. Parallel chunks mean parallel packets can be processed in parallel. Packets are the unit of data transfer within network and parallelism below that is the network’s job. So the ACE memory management and control unit are designed to ensure using all algorithmic parallelism opportunities that we will describe next.

4.3.1 Memory Management

The SRAM within ACE is partitioned according to the number of phases of the collective algorithm being, each serves as the source for one specific phase. In addition, one final partition is added that holds the final results for RX DMA. For e.g., the ring-based all-reduce has 1 phase and hence needs 2 partitions, as discussed in [Section 4.2](#). More complex hierarchical topologies can implement the collectives over multiple phases [40]. one or more state machines coordinate the dataflow within ACE for each phase.

Chunks are brought from main memory to the first phase partition within SRAM by TX DMA using a pipeline manner. Chunks reside within SRAM and moves to next partitions as they go to later phases of collective algorithm. Finally, after finishing the last phase, the result is sent back to the main memory by RX DMA.

An alternative approach is to allocate a constant space for a chunk and use that space during all phases of the collective. However, this is not an efficient way of using valuable on-chip storage due to one important property of collective operations: the data size might change during different phases of the algorithm. Thus, allocating a constant space wastes on-chip storage or requires sophisticated dynamic allocation/de-allocation schemes to manage free spaces, adding complexity to both datapath and control unit.

Using logical partitions for different phases allows for a fine-grained yet low complexity storage allocation/de-allocation scheme as chunks go through different phases, as well as simplifying the control logic. The partitions size can be then be adjusted according to the requirement of each phase that is dependant on the algorithm and network speed for that phase (in case of having links with different speeds).

4.3.2 Control Unit

The control unit comprises of multiple programmable state machines. Each state machine can be programmed for a specific phase of a specific collective algorithm, and holds a queue of chunks that should process in order. Each entry of this queue holds the *context* of a chunk like its start and end address inside the SRAM and the address range for holding the final result for next phase. When a chunk is created in ACE, it is also assigned the state machines it should go through for each phase⁷. When entering each phase, the chunk is inserted into the queue of its assigned state machine for that phase. The state machines then compete with each other to access different resources, resulting in overlapping

⁷It is possible that, for a given workload, different collective operations (e.g. all-reduce and all-to-all) exist for the same phase. In this case, the state machines allocated for that phase should be programmed to handle all collective operations for that phase

and out-of-order execution of multiple chunks both within and across phases. This increases resource utilization and network bandwidth. The available parallelism is only bounded by the number of available state machines to manage the dataflow for each phase.

4.4 Interface with NPU and NIC

ACE extends the existing NIC interface exposed to NPU as shown in [Fig. 6](#). NIC control forwards the ACE specific commands from NPU/ACE to ACE/NPU. The NPU-NIC command interface is similar to UCX [43] or OFI [18] which are the standard high level NIC interfaces. Once collective command is received, ACE decides when to load data given the availability of SRAM space. Finally, ACE notifies the completion of chunk collective by raising an interrupt and forwarding it to NPU.

In addition, ACE control unit should consult NIC control unit to ensure available space before attempting to write to NIC SRAM. Moreover, NIC should be able to detect whether the incoming packets belongs to normal mode or ACE activated mode. This is done by including a bit in packet headers to distinguish between the two modes.

4.5 Flexibility and Scalability

Recall from [Section 2](#), there can be different classes of collectives depending on the parallelism approach, collective algorithm, and network topology. As DNNs evolve, their training systems need to be able to evolve as well to run any collective over any topology. The microarchitecture of ACE is designed keeping this goal in mind.

Supporting Different Collectives. The general principles for running any collective algorithm using ACE remain the same. For a collective with say P phases, the SRAM is divided to $P+1$ partitions. Each partition is assigned to a phase, as described in [Section 4.3.1](#) and state-machines as described in [Section 4.3.2](#). The only difference between different collective algorithms is that the state machines should be programmed to perform that specific algorithm.

Supporting Different Topologies. Since ACE handles the collectives at the endpoints, it is orthogonal to any network topology (e.g. switch-based, point-to-point, hybrid). From the logical view, ACE can perform any collective algorithm (e.g. ring-based all-reduce) on top of any physical topology. It is then the job of network protocol and routing algorithm to deliver the packets accordingly⁸.

5. EVALUATION METHODOLOGY

This section describes our methodology establishing and simulating high-performance training systems and evaluating the benefits of communication acceleration.

Target Training Platforms. We model future DL training platforms comprising of multiple NPUs integrated through multi-chip packaging technology [10] on a package, and multiple packages interconnected via a dedicated scale-up fabric. Given the large design space, we limit the fabric topologies in this study to a 3D Torus (inspired by Google’s TPU platform [26]) and fully connected cross-bar switch

⁸Note that ACE is compatible with networks with out-of-order packet delivery

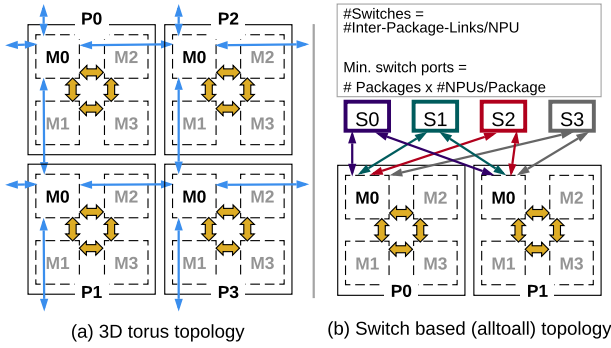


Figure 8: Target Systems: 3D Torus and Fully-connected Switch Topology. Multiple NPU chips (M_0, \dots) are connected within a package, and multiple packages (P_0, \dots) are connected together, presenting heterogeneous scale-up bandwidth across the system. Connectivity is shown for NPU M_0 . NPU's $M_1/M_2/M_3$ have similar connectivity - not shown.

Table 5: Topology details

Topology/ Dimension Notation	Collective Algorithm	BW/Dimension
3D torus / $L \times V \times H$ (L is the # of NPUs within a package, V is the # of inter-package rows, H is the # of inter-package columns)	Hierarchical all-reduce: 1. Ring-based reduce-scatter in L 2. Ring-based all-reduce in V 3. Ring-based all-reduce in H 4. Ring-based all-gather in L Hierarchical all-to-all: 1. Ring-based all-to-all in L 2. Ring-based all-to-all in V 3. Ring-based all-to-all in H NOTE: If $V/L=1$, then L/V has 2 bi-directional rings.	1 bi-directional ring in L (using 2 intra-package links/NPU), 1 bi-directional ring in V (using 2 inter-package links/NPU), 1 bi-directional ring in H (using 2 inter-package links/NPU)
Alltoall/ $L \times P$ (L is the # of NPUs within a package, P is the # of packages)	Hierarchical all-reduce: 1. Ring-based reduce-scatter in L 2. Direct all-reduce in P 3. Ring-based all-gather in L Hierarchical all-to-all: 1. Ring-based all-to-all in L 2. Direct all-to-all in P	1 bidirectional ring in L (using 2 intra-package links/NPU), 4 fully connected switches (using 4 inter-package links/NPU)

(inspired by NVIDIA's DGX-2 platform [36]). Fig. 8 shows the two selected topologies.

Table 5 shows more details about the topologies such as: the notation used to define their dimension, the collective algorithms they are using per dimension, and how intra-package/inter-package links are used to construct rings or connect to switches.

Target Collective Algorithms. As shown in Table 5, we use hierarchical multi-phase collective algorithms for our multi-dimensional physical topologies [40]. Each phase uses a simple ring-based or direct algorithm depending on the topology for that dimension. The ring-based all-reduce (as well as ring-based reduce-scatter and all-gather) was described in Section 4.2. In order to perform direct all-reduce for N nodes, the chunk is broken into N (or multiple of N as described earlier) messages and the i 'th node is responsible for reduction of i 'th message. Hence, all nodes send their i 'th messages to node i simultaneously. After receiving all i 'th messages, node i performs the reduction and then, simultaneously broadcast its message to all other nodes.

Direct all-to-all is simple since each node simply sends all of the respective messages to their destination nodes at the same time. Ring-based all-to-all of N nodes consists of $N-1$ steps where step s , each node sends a message that belongs to the node with distance s in the ring.

Table 6: Synthesis Results

Component	Area (μm^2)	Power (mW)
ALU	16112	7.552
Control unit	159803	128
4x1MB SRAM banks	5113696	4096
Crossbar switches	1084	0.329
ACE (Total)	5339031	4255

Table 7: System parameters

Parameter	Values
Intra-Package	
Packet size	256 Bytes
Per link BW	200 GB/s
Link latency	90 cycles
# of links/NPU	2
Link efficiency	94%
Inter-Package	
Packet size	256 bytes
Per link BW	25 GB/s
Link latency	200 cycles
# of links/NPU	4 (bi-directional)
Link efficiency	94%
NPU and NIC parameters	
Compute Accel.	256x256 TPU-like
NPU-NIC BW	500 GB/s
NPU-MEM BW	900 GB/s
Message size	4KB

Shared Memory. We assume a shared memory model across the scale-up fabric in our target platforms, similar to NVIDIA DGX-2 [36]. This design decision is reasonable for two reasons: first, optimizing for *Non-Uniform Memory Access* (NUMA) and shared memory is challenging - as evident from extensive work on HPC workloads for CPUs. Additionally, having two separate communication paths, i.e. say shared memory within package and message passing across packages, will increase the scheduling and optimization complexity for various collective algorithms. Therefore, we assume explicit communication between NPUs both within a package and across, through a high-performance topology aware communication library. This programming model also allows scaling the number of modules within a package with improvements in packaging technology [6].

Simulation Parameters. Table 7 shows the major system parameters. To model the network communication and latency, we used ASTRA-SIM [40], a distributed DNN training simulator, and developed ACE on top of that. For the compute model, we used the SCALE-SIM [41] to find the compute times (i.e. forward-pass, weight gradient, and input gradient) of the workloads. The compute model is a 700MHz 256x256 systolic array to be an estimate for the 4x128x128 systolic array of the TPU-V3 chip. This means ~ 91.5 TFLOPS compute power per node that is quite comparable to the state-of-the-art training platforms [33]. For modeling the bus (i.e. NPU-NIC and NPU-Mem) congestion, we used the LogGP [9] model with $L=50$ and $o=g=20$ cycles (these values are within the range stated in [20]), and G equals to the corresponding BW of the NPU-NIC and NPU-Mem bus, as stated in Table 7.

NPU-Mem bandwidth is chosen based on NVIDIA Volta [24]. NPU-NIC bandwidth is assumed to be the sum of all intra-package/inter-package links as a logical choice to prevent NPU-NIC bandwidth to be the bottleneck in driving

the network links. Inter-package link BW is assumed to be the same as NVlink [29], while intra-pakcage bandwidth is selected based on [44] that is an expected bandwidth for high performance multi-chip package systems.

Target Systems. We considered four different systems:

- **Baseline:** Represents a conventional system where the NPU is responsible performing the collective communication. Based on our analysis from [Section 3](#), we conservatively assume $\sim 5\%$ of the compute and $\sim 20\%$ of the Mem BW is spent for collective communication.
- **Baseline++:** Considers a baseline system with higher compute and memory bandwidth than Baseline such that the available NPU compute and memory bandwidth is same as ACE. However, the actual communication still occurs via the Memory and NIC like the Baseline. This baseline helps us isolate the effects of latency and congestion over the NPU-MEM and NPU-NIC buses.
- **ACE:** Implements our proposed system. In this case, 100% of the NPU resource is dedicated to the training algorithm. Moreover, memory BW is only used for initial load and final writeback to/from ACE. Hence, we assume only 5% of the memory BW available to ACE.
- **Ideal:** It is a system where the NIC has unlimited resources and is able to handle all collective communication operations using one cycle. This essentially means that there is no associated latency from the endpoint side in the collective communication algorithm. This gives an upper bound to our design. In this case 100% of compute and memory is allocated for training algorithm only.

Target Workloads. In order to evaluate our platforms, we considered two different sets of workloads: (1) Microbenchmarks that consist of the single all-reduce or all-to-all collective communications, and (2) ResNet-50 [19] and GNMT [48] DNNs. For the DNNs, we consider data-parallel parallelism (i.e. requiring all-reduce for weight gradients) for two training iterations with Last-In-First-Out (LIFO) collective scheduling policy to give more priority to the collectives of first layers during back-propagation. The mini-batch size is set to be 32 per node for both workloads. We demonstrate our design with both end-to-end runtime and detailed per-layer breakdown.

6. RESULTS

This section presents simulation results comparing ACE against *ideal* and *baseline* for micro-benchmarks (i.e. single collective performance) and for real workloads. But first we present area/power analysis of ACE on 28nm technology nod.

ACE: Area/Power Analysis. We ran a number of simulations to discover the best yet reasonably low overhead parameters for ACE. Due to space reasons, we do not present the design space evaluation for ACE but here present the parameters we chose. We found out that a $4 \times 1\text{MB}$ SRAM banks and 16 state machines are sufficient to implement and drive our target networks and algorithms. The complexity of each state machine is approximated by 8KB SRAM that is sufficient to implement various target algorithms. Also, 4 wide ALU units, each consisting of 16x FP32 functional units were sufficient for ACE. The interconnect between SRAM

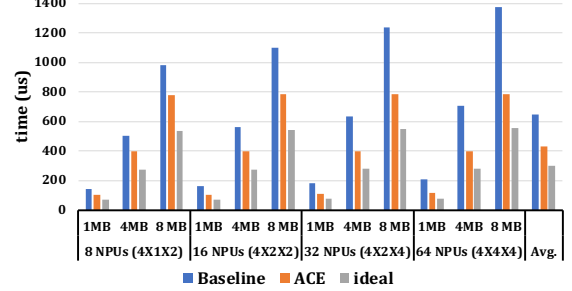


Figure 9: Baseline, ACE and Ideal total communication latency (μs) of the all-reduce collective for the torus topology.

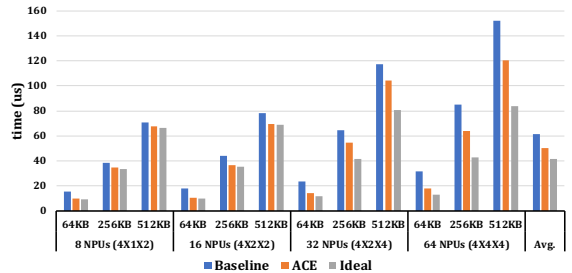


Figure 10: Baseline, ACE and Ideal total communication latency (μs) of the all-to-all collective for the torus topology.

and functional units are wide 64B buses. We implemented ACE using Verilog and synthesized the design using the Synopsis Design Compiler in 28nm technology node. [Table 6](#) shows the area and power estimates for our design, enumerating individual components as well as ACE itself. Compared to the area and power of high-end training accelerators reported in [26, 47], ACE has less than 2% overhead in both area and power.

In addition, we used a simple heuristic for SRAM partitioning that partitions the SRAM based on the (available network bandwidth \times initial chunk size) for each phase⁹. Moreover, state machines are evenly distributed across different phases.

Micro-benchmarks. In this section, we test the performance of baseline, ACE and Ideal for single all-reduce and all-to-all collectives¹⁰.

[Fig. 9](#) presents the ideal, baseline, and ACE all-reduce on 2D/3D Torus topologies. On average, using ACE improves the total communication latency by $1.51\times$ compared to the baseline. Ideal is only $1.43\times$ better than ACE, while compared to baseline, Ideal is $2.17\times$ better.

To delve deeper into the reason of this improvement, [Fig. 11](#) shows the detailed time breakdown for [Fig. 9](#). As shown in the figure, due to better performance, the average chunk queuing is reduced by 44.9% on average in ACE compared to the baseline. In addition, ACE significantly reduces the bus congestion (total NIC-NPU/Mem-NIC bus queuing + transfer) by 88.9% on average compared to the baseline. Note that in general the message network transfer in ACE is smaller

⁹For example, a phase with $2 \times$ link bandwidth and $2 \times$ initial chunk size has a partition $4 \times$ greater than a phase with $1 \times$ bandwidth and $1 \times$ chunk size. Also note that if for each phase, there are different chunk sizes belonging to different collective operations, we use average of such chunk sizes.

¹⁰All-reduce is the only collective communication operation in most of the training workloads. However, sometimes all-to-all is used especially for recommendation model DNNs where all-to-all is used for embeddings.

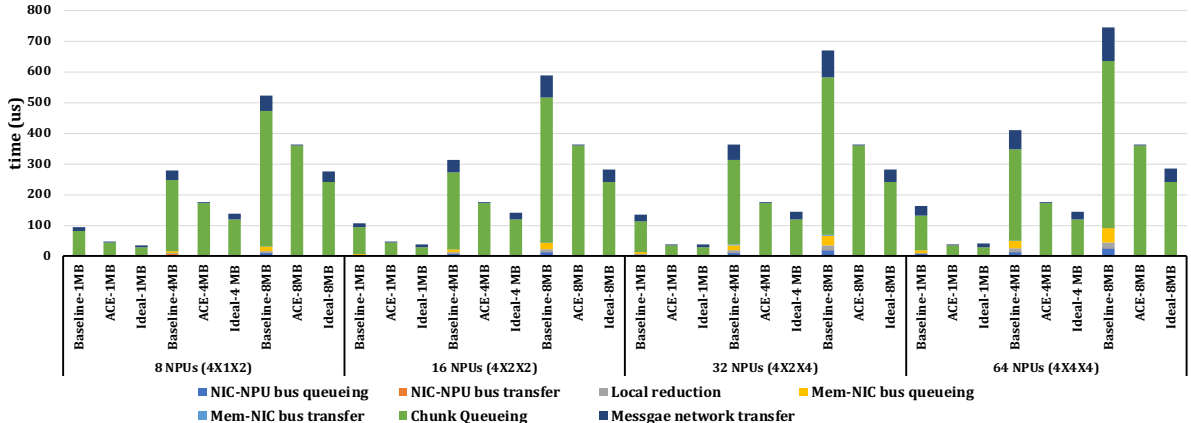


Figure 11: The detailed latency breakdown for all-reduce on torus network. The **NIC-NPU/Mem-NIC bus queuing** and **bus transfer** shows the average queuing and average transfer time of transfer requests in NIC-NPU/Mem-NIC bus, respectively. The **local reduction** delay refers to the average latency of messages being reduced by the NPU. **Chunk queuing** is the average amount of time chunks are waiting for the chunks that are ahead of them to be finished and then start executing. **Message network transfer** refers to the average amount of time messages spend in the network.

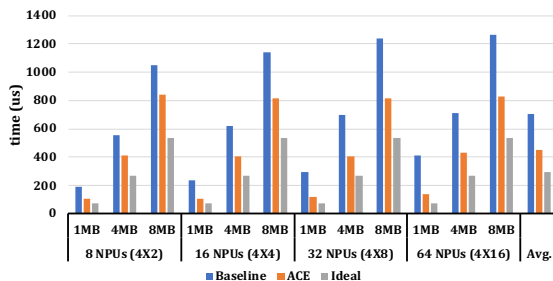


Figure 12: Baseline, ACE and Ideal total communication latency (μ s) of the all-reduce collective for the alioall topology.

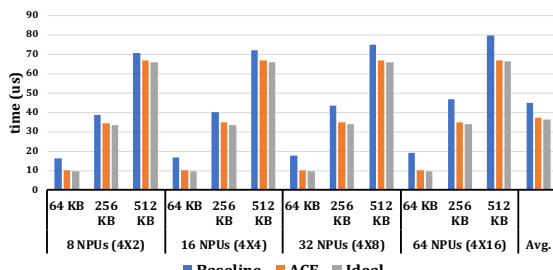


Figure 13: Baseline, ACE and Ideal total communication latency (μ s) of the all-to-all collective for the alioall topology

than baseline/ideal systems because in ACE, chunk sizes (and hence message sizes) are smaller because of the limited on-chip SRAM. However, as Fig. 11 and Fig. 9 show, this limitation does not prevent ACE from driving the network in a much more efficient way compared to the baseline.

We observe the same behavior in other collectives and systems. Fig. 10, Fig. 12, and Fig. 13 show the performance of the three systems for all-to-all on torus, all-reduce on alioall, and all-to-all on alioall, respectively. On average ACE improves all-to-all on torus by $1.22\times$, all-reduce on alioall by $1.55\times$ and all-to-all on alioall by $1.20\times$, compared to the baseline system.

Workload performance comparison. In this section, we evaluated the four different systems mentioned in Section 5. Fig. 14 shows the total training loop algorithm latency for two iterations of the ResNet-50 DNN training loop running on different torus network sizes. Each latency is decomposed into

endpoint delay (compute+bus congestion) and the exposed communication latency delay. The exposed communication latency is the latency that the training algorithm is forced to stop because of waiting for the communication. On average, ACE improves the overall training latency by $2.71\times$ compared to the baseline.

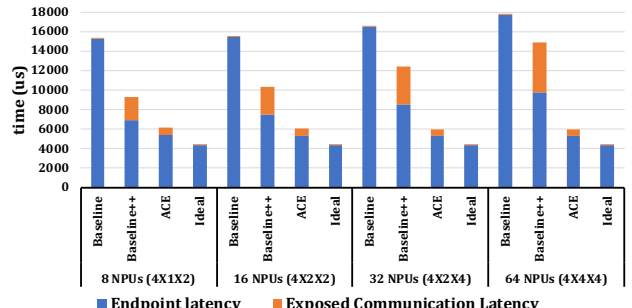


Figure 14: The baseline, baseline++, ACE and ideal latency (μ s) for two training iterations of ResNet-50 training algorithm running on torus topologies. Note that endpoint latency contains congestion latencies as well.

Fig. 15 shows the layer wise exposed latency and its comparison with compute latency for baseline++ and ACE systems for the 64 NPU case. As the figure shows, only switching from baseline to baseline++ does not completely address the limitations NPU centric communication handling approach and there is still a significant bottleneck arising from congestion in the buses that are mostly mitigated in ACE. This difference becomes more evident by looking at the later layers of the ResNet-50 in Fig. 15 that have larger communication sizes. We note that this is not the indication that the poor performance of the baseline in general. In fact, as shown in Fig. 14, a training iteration duration is ~ 9 ms for the 64-node baseline system. This means that one epoch of training on the ImageNet dataset [12] takes ~ 61.5 seconds that is comparable to the best training performance-per-node times reported [33]. However, Fig. 14 points to the available opportunity to further improve the performance since high performance NPUs: (i) leave less time to overlap the communication with computation and (ii) require more collectives to be executed in parallel, resulting in more bus congestion

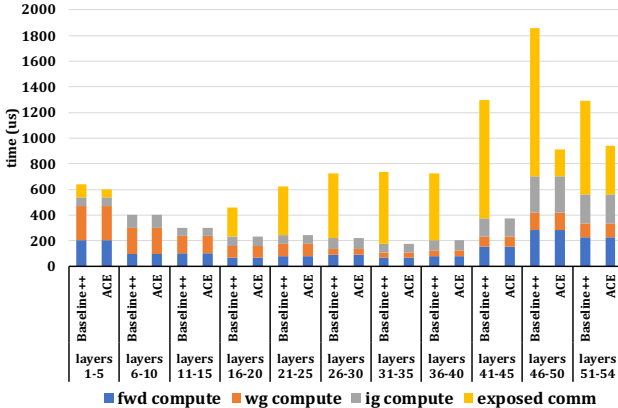


Figure 15: The layer wise exposed communication latency (μ s) and its comparison with compute (excluding bus congestion) latency for baseline++ and ACE running on the 64-NPU (4X4X4) system. The latencies are for 2 training iterations.

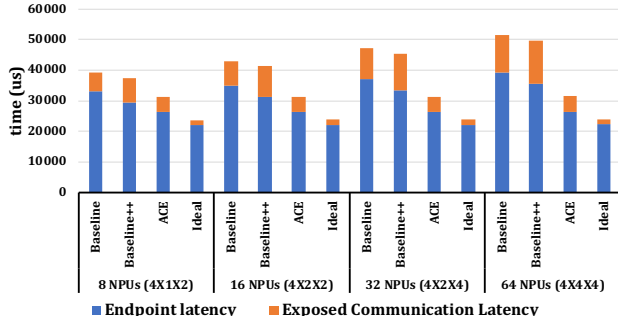


Figure 16: The baseline, baseline++, ACE and ideal latency (μ s) for two training iterations of GNMT training algorithm running on torus topologies. Note that endpoint latency contains congestion latencies as well.

and queuing for compute and memory resources.

Fig. 16 shows the total endpoint and exposed delays for GNMT running on torus topology. On average, ACE achieves $1.44 \times$ better performance compared to the baseline. Baseline++ only works $1.04 \times$ better than baseline.

Finally, Fig. 17 compares the network bandwidth utilization of baseline, baseline++ and ACE normalized to their respective ideal systems for both ResNet-50 and GNMT networks. On average, ACE improves the bandwidth utilization by $1.97 \times$, increasing the bandwidth utilization to 74.6% of the ideal system compared to the baseline that drives 37.8% of ideal system network bandwidth.

7. RELATED WORK

Previous work have demonstrated the efficiency of collective offload to either smart NICs or network switches. As explained in Table 1, ACE is a SmartNIC for accelerator-based systems and can be integrated in different system topologies such as switch based or point-to-point (e.g. Torus) systems.

SmartNICs and Communication offload Prior SmartNIC solutions for collective offload, such as [46, 20], focused on scale-out networks and HPC workloads. Triggered collectives [46] is the closest comparison to ACE but is specific to Portals transport and CPU-based scale-out systems while ACE is transport-agnostic and sufficiently flexible to support hierarchical topologies (local + scale-up). Unlike both Triggered collectives [46] and ACE, sPIN [20] uses ARM cores and will not be able to drive high bandwidths required for DL

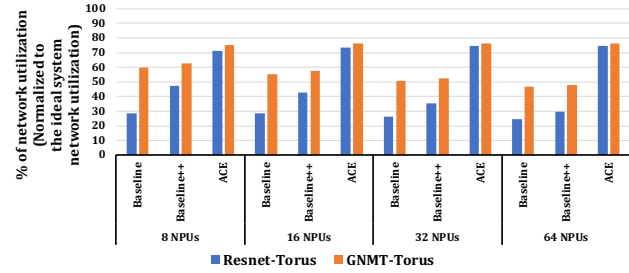


Figure 17: The baseline, baseline++ and ACE network bandwidth utilization for ResNet-50 and GNMT normalized to their respective ideal system bandwidth utilization

platforms. INCEPTIONN [31] proposes a Smart-NIC based compression offload for parameter servers for DL training. The inherent differences between parameter server vs. collectives makes ACE vs. INCEPTIONN comparison out of scope for this paper. HPC systems with Torus-based topology, such as BlueGene [27], PERCS [39], and Anton2 [17], have supported collective offload on network routers. SmartNICs are more flexible than routers found in such system since routers are purpose-built for the target topology.

Numerous other proposals have demonstrated the benefits of SmartNICs for communication offload but do not address the requirements of DL training. Microsoft’s Brainwave [14] proposes a bump-in-the-wire SmartNIC for distributed inference. IncBricks [32] proposes distributed in-network caches on the scale-out network, which store key-value pairs for frequently accessed data. They allow simple operations such as increment to be done using a simple in-network processor. NetCache [25] uses the ASIC within a switch to do dynamic caching and load-balancing of requests to that switch.

Switch-based collective offload Switch-based offload solutions, such Intel’s Barefoot [1], Mellanox SHARP [3], and NVIDIA’s shared memory switch offload [13], have proposed aggregation in switches. In contrast to SmartNIC-based collective offload solutions, Switch-based solutions have two major disadvantages: (1) they are inherently limited to switch topologies while SmartNICs are more flexible and support point-to-point (e.g. Torus) and switch topology, (2) they have higher constraints on compute and memory resources given the large number of endpoints connecting to the switch. SmartNIC based solutions overcome this by distributing the resource requirement across endpoints. More specifically, Barefoot [1] offload scheme requires operating on quantized integer values (due to lack of floating point arithmetic in the switch) potentially affecting training accuracy for future DL models. On the other hand, NVIDIA’s switch-based offload [13] is purpose-built for shared memory allreduce collectives; limiting the number of endpoints and types of collectives that can be supported. Switch offload has also been explored for accelerating Reinforcement learning [30].

8. CONCLUSIONS

One oft ignored aspects of scaling distributed DL training systems is the complex interplay between (a) the processing engines used for executing DL compute operations such as GEMMs/Convolutions versus executing collective communication, and (b) the contention between them for shared resources like memory bandwidth. In this paper, we propose a novel micro-architecture, called ACE to augment NICs for

DL collective communication offload to efficiently drive the hierarchical scale-up fabric and free up critical compute and memory resources for DL computation. We demonstrate ACE achieves $2.71\times$ and $1.44\times$ speedup for modern DL workloads such as ResNet-50 and GNMT over the state-of-the-art bandwidth-equivalent baseline, respectively.

9. REFERENCES

- [1] [Online]. Available: <https://www.barefootnetworks.com/>
- [2] [Online]. Available: <https://github.com/UoB-HPC/BabelStream>
- [3] *Mellanox Scalable Hierarchical Aggregation and Reduction Protocol (SHARP)*. [Online]. Available: <https://www.mellanox.com/products/sharp>
- [4] M. Abadi, A. Agarwal, P. Barham, E. Brevdo, Z. Chen, C. Citro, G. S. Corrado, A. Davis, J. Dean, M. Devin, S. Ghemawat, I. Goodfellow, A. Harp, G. Irving, M. Isard, Y. Jia, R. Jozefowicz, L. Kaiser, M. Kudlur, J. Levenberg, D. Mané, R. Monga, S. Moore, D. Murray, C. Olah, M. Schuster, J. Shlens, B. Steiner, I. Sutskever, K. Talwar, P. Tucker, V. Vanhoucke, V. Vasudevan, F. Viégas, O. Vinyals, P. Warden, M. Wattenberg, M. Wicke, Y. Yu, and X. Zheng, “TensorFlow: Large-scale machine learning on heterogeneous systems,” 2015, software available from tensorflow.org. [Online]. Available: <http://tensorflow.org/>
- [5] D. Amodei and D. Hernandez, “Ai and compute,” 2018. [Online]. Available: <https://openai.com/blog/ai-and-compute/>
- [6] A. Arunkumar, E. Bolotin, B. Cho, U. Milic, E. Ebrahimi, O. Villa, A. Jaleel, C.-J. Wu, and D. Nellans, “Mcm-gpu: Multi-chip-module gpus for continued performance scalability,” in *Proceedings of the 44th Annual International Symposium on Computer Architecture*, ser. ISCA ’17. New York, NY, USA: ACM, 2017, pp. 320–332. [Online]. Available: <http://doi.acm.org/10.1145/3079856.3080231>
- [7] E. Chan, R. van de Geijn, W. Gropp, and R. Thakur, “Collective communication on architectures that support simultaneous communication over multiple links,” in *Proceedings of the Eleventh ACM SIGPLAN Symposium on Principles and Practice of Parallel Programming*, ser. PPoPP ’06. New York, NY, USA: ACM, 2006, pp. 2–11. [Online]. Available: <http://doi.acm.org/10.1145/1122971.1122975>
- [8] M. Cho, U. Finkler, S. Kumar, D. S. Kung, V. Saxena, and D. Sreedhar, “Powerai DDL,” *CoRR*, vol. abs/1708.02188, 2017. [Online]. Available: <http://arxiv.org/abs/1708.02188>
- [9] D. Culler, R. Karp, D. Patterson, A. Sahay, K. E. Schausler, E. Santos, R. Subramonian, and T. von Eicken, “Logp: Towards a realistic model of parallel computation,” in *Proceedings of the Fourth ACM SIGPLAN Symposium on Principles and Practice of Parallel Programming*, ser. PPoPP ’93. New York, NY, USA: ACM, 1993, pp. 1–12. [Online]. Available: <http://doi.acm.org/10.1145/155332.155333>
- [10] W. J. Dally, C. T. Gray, J. Poulton, B. Khailany, J. Wilson, and L. Dennison, “Hardware-enabled artificial intelligence,” in *2018 IEEE Symposium on VLSI Circuits*, June 2018, pp. 3–6.
- [11] D. Das, S. Avancha, D. Mudigere, K. Vaidyanathan, S. Sridharan, D. D. Kalamkar, B. Kaul, and P. Dubey, “Distributed deep learning using synchronous stochastic gradient descent,” *CoRR*, vol. abs/1602.06709, 2016. [Online]. Available: <http://arxiv.org/abs/1602.06709>
- [12] J. Deng, W. Dong, R. Socher, L.-J. Li, K. Li, and L. Fei-Fei, “ImageNet: A Large-Scale Hierarchical Image Database,” in *CVPR09*, 2009.
- [13] B. K. et al., “An in-network architecture for accelerating shared-memory multiprocessor collectives,” in *2020 ACM/IEEE 47th Annual International Symposium on Computer Architecture (ISCA)*, 2020. [Online]. Available: <https://www.iscaconf.org/isca2020/papers/466100a996.pdf>
- [14] J. Fowers, K. Ovtcharov, M. Papamichael, T. Massengill, M. Liu, D. Lo, S. Alkalay, M. Haselman, L. Adams, M. Ghandi, S. Heil, P. Patel, A. Sapek, G. Weisz, L. Woods, S. Lanka, S. K. Reinhardt, A. M. Caulfield, E. S. Chung, and D. Burger, “A configurable cloud-scale dnn processor for real-time ai,” in *2018 ACM/IEEE 45th Annual International Symposium on Computer Architecture (ISCA)*, 2018, pp. 1–14.
- [15] P. Goyal, P. Dollár, R. B. Girshick, P. Noordhuis, L. Wesolowski, A. Kyrola, A. Tulloch, Y. Jia, and K. He, “Accurate, large minibatch SGD: training imagenet in 1 hour,” *CoRR*, vol. abs/1706.02677, 2017. [Online]. Available: <http://arxiv.org/abs/1706.02677>
- [16] R. L. Graham, D. Bureddy, P. Lui, H. Rosenstock, G. Shainer, G. Bloch, D. Goldenerg, M. Dubman, S. Kotchubievsky, V. Koushmir, L. Levi, A. Margolin, T. Ronen, A. Shpiner, O. Wertheim, and E. Zahavi, “Scalable hierarchical aggregation protocol (sharp): A hardware architecture for efficient data reduction,” in *2016 First International Workshop on Communication Optimizations in HPC (COMHPC)*, 2016, pp. 1–10.
- [17] J. P. Grossman, B. Towles, B. Greskamp, and D. E. Shaw, “Filtering, reductions and synchronization in the anton 2 network,” in *2015 IEEE International Parallel and Distributed Processing Symposium*, 2015, pp. 860–870.
- [18] P. Grun, S. Hefty, S. Sur, D. Goodell, R. D. Russell, H. Pritchard, and J. M. Squyres, “A brief introduction to the openfabrics interfaces - a new network api for maximizing high performance application efficiency,” in *2015 IEEE 23rd Annual Symposium on High-Performance Interconnects*, 2015, pp. 34–39.
- [19] K. He, X. Zhang, S. Ren, and J. Sun, “Deep residual learning for image recognition,” *CoRR*, vol. abs/1512.03385, 2015. [Online]. Available: <http://arxiv.org/abs/1512.03385>
- [20] T. Hoefer, S. D. Girolamo, K. Taranov, R. E. Grant, and R. Brightwell, “spin: High-performance streaming processing in the network,” *CoRR*, vol. abs/1709.05483, 2017. [Online]. Available: <http://arxiv.org/abs/1709.05483>
- [21] Intel, “Intel caffe,” 2018. [Online]. Available: <https://github.com/intel/caffe>
- [22] Intel, “Intel machine learning scalability library (mlsl),” 2018. [Online]. Available: <https://github.com/intel/MLSL>
- [23] Intel, “Intel nervana graph,” 2018. [Online]. Available: <https://github.com/NervanaSystems/ngraph>
- [24] Z. Jia, M. Maggini, B. Staiger, and D. P. Scarpazza, “Dissecting the NVIDIA volta GPU architecture via microbenchmarking,” *CoRR*, vol. abs/1804.06826, 2018. [Online]. Available: <http://arxiv.org/abs/1804.06826>
- [25] X. Jin, X. Li, H. Zhang, R. Soulé, J. Lee, N. Foster, C. Kim, and I. Stoica, “Netcache: Balancing key-value stores with fast in-network caching,” in *Proceedings of the 26th Symposium on Operating Systems Principles*, ser. SOSP ’17. New York, NY, USA: Association for Computing Machinery, 2017, p. 121–136. [Online]. Available: <https://doi.org/10.1145/3132747.3132764>
- [26] N. P. Jouppi, C. Young, N. Patil, D. A. Patterson, G. Agrawal, R. Bajwa, S. Bates, S. Bhatia, N. Boden, A. Borchers, R. Boyle, P. Cantin, C. Chao, C. Clark, J. Coriell, M. Daley, M. Dau, J. Dean, B. Gelb, T. V. Ghaemmaghami, R. Gottipati, W. Gulland, R. Hagmann, R. C. Ho, D. Hogberg, J. Hu, R. Hundt, D. Hurt, J. Ibarz, A. Jaffey, A. Jaworski, A. Kaplan, H. Khaitan, A. Koch, N. Kumar, S. Lacy, J. Laudon, J. Law, D. Le, C. Leary, Z. Liu, K. Lucke, A. Lundin, G. MacKean, A. Maggiore, M. Mahony, K. Miller, R. Nagarajan, R. Narayanaswami, R. Ni, K. Nix, T. Norrie, M. Omernick, N. Penukonda, A. Phelps, J. Ross, A. Salek, E. Samadiani, C. Severn, G. Sizikov, M. Snelham, J. Souter, D. Steinberg, A. Swing, M. Tan, G. Thorson, B. Tian, H. Toma, E. Tuttle, V. Vasudevan, R. Walter, W. Wang, E. Wilcox, and D. H. Yoon, “In-datacenter performance analysis of a tensor processing unit,” *CoRR*, vol. abs/1704.04760, 2017. [Online]. Available: <http://arxiv.org/abs/1704.04760>
- [27] D. J. Kerbyson, K. J. Barker, A. Vishnu, and A. Hoisie, “A performance comparison of current hpc systems: Blue gene/q, cray xe6 and infiniband systems,” *Future Generation Computer Systems*, vol. 30, pp. 291 – 304, 2014, special Issue on Extreme Scale Parallel Architectures and Systems, Cryptography in Cloud Computing and Recent Advances in Parallel and Distributed Systems, ICPADS 2012 Selected Papers. [Online]. Available: <http://www.sciencedirect.com/science/article/pii/S0167739X13001337>
- [28] N. S. Keskar, D. Mudigere, J. Nocedal, M. Smelyanskiy, and P. T. P. Tang, “On large-batch training for deep learning: Generalization gap and sharp minima,” *CoRR*, vol. abs/1609.04836, 2016. [Online]. Available: <http://arxiv.org/abs/1609.04836>
- [29] A. Li, S. L. Song, J. Chen, J. Li, X. Liu, N. R. Tallent, and K. J. Barker, “Evaluating modern GPU interconnect: Pcie, nvlink, nv-sli, nvswitch and gpudirect,” *CoRR*, vol. abs/1903.04611, 2019. [Online].

Available: <http://arxiv.org/abs/1903.04611>

[30] Y. Li, I.-J. Liu, Y. Yuan, D. Chen, A. Schwing, and J. Huang, "Accelerating distributed reinforcement learning with in-switch computing," in *Proceedings of the 46th International Symposium on Computer Architecture*, ser. ISCA '19. New York, NY, USA: Association for Computing Machinery, 2019, p. 279–291. [Online]. Available: <https://doi.org/10.1145/3307650.3322259>

[31] Y. Li, J. Park, M. Alian, Y. Yuan, Z. Qu, P. Pan, R. Wang, A. Schwing, H. Esmaeilzadeh, and N. Kim, "A network-centric hardware/algorithm co-design to accelerate distributed training of deep neural networks," 10 2018, pp. 175–188.

[32] M. Liu, L. Luo, J. Nelson, L. Ceze, A. Krishnamurthy, and K. Atreya, "Inbricks: Toward in-network computation with an in-network cache," in *Proceedings of the Twenty-Second International Conference on Architectural Support for Programming Languages and Operating Systems*, ser. ASPLOS '17. New York, NY, USA: Association for Computing Machinery, 2017, p. 795–809. [Online]. Available: <https://doi.org/10.1145/3037697.3037731>

[33] H. Mikami, H. Suganuma, P. U.-Chupala, Y. Tanaka, and Y. Kageyama, "Imagenet/resnet-50 training in 224 seconds," *CoRR*, vol. abs/1811.05233, 2018. [Online]. Available: <http://arxiv.org/abs/1811.05233>

[34] M. Naumov, D. Mudigere, H. M. Shi, J. Huang, N. Sundaraman, J. Park, X. Wang, U. Gupta, C. Wu, A. G. Azzolini, D. Dzhulgakov, A. Mallevich, I. Cherniavskii, Y. Lu, R. Krishnamoorthi, A. Yu, V. Kondratenko, S. Pereira, X. Chen, W. Chen, V. Rao, B. Jia, L. Xiong, and M. Smelyanskiy, "Deep learning recommendation model for personalization and recommendation systems," *CoRR*, vol. abs/1906.00091, 2019. [Online]. Available: <http://arxiv.org/abs/1906.00091>

[35] NVIDIA, "Nvidia collective communications library (nccl)," 2018. [Online]. Available: <https://developer.nvidia.com/nccl>

[36] NVIDIA, "Nvidia dgx-2," 2019. [Online]. Available: <https://www.nvidia.com/en-us/data-center/dgx-2/>

[37] S. Ouyang, D. Dong, Y. Xu, and L. Xiao, "Communication optimization strategies for distributed deep learning: A survey," 2020.

[38] P. Patarasuk and X. Yuan, "Bandwidth optimal all-reduce algorithms for clusters of workstations," *J. Parallel Distrib. Comput.*, vol. 69, no. 2, pp. 117–124, Feb. 2009. [Online]. Available: <http://dx.doi.org/10.1016/j.jpdc.2008.09.002>

[39] R. Rajamony, L. B. Arimilli, and K. Gildea, "Percs: The ibm power7-ih high-performance computing system," *IBM J. Res. Dev.*, vol. 55, no. 3, p. 233–244, May 2011. [Online]. Available: <https://doi.org/10.1147/JRD.2011.2109230>

[40] S. Rashidi, S. Sridharan, S. Srinivasan, and T. Krishna, "ASTRA-SIM: Enabling SW/HW Co-Design Exploration for Distributed DL Training Platforms," in *IEEE International Symposium on Performance Analysis of Systems and Software, ISPASS 2020, Boston, MA, USA, August 22–26, 2020*. IEEE, 2020. [Online]. Available: https://synergy.ece.gatech.edu/wp-content/uploads/sites/332/2020/03/astrasim_ispass2020.pdf

[41] A. Samajdar, Y. Zhu, P. N. Whatmough, M. Mattina, and T. Krishna, "Scale-sim: Systolic CNN accelerator," *CoRR*, vol. abs/1811.02883, 2018. [Online]. Available: <http://arxiv.org/abs/1811.02883>

[42] A. Sapio, M. Canini, C. Ho, J. Nelson, P. Kalnis, C. Kim, A. Krishnamurthy, M. Moshref, D. R. K. Ports, and P. Richtárik, "Scaling distributed machine learning with in-network aggregation," *CoRR*, vol. abs/1903.06701, 2019. [Online]. Available: <http://arxiv.org/abs/1903.06701>

[43] P. Shamis, M. G. Venkata, M. G. Lopez, M. B. Baker, O. Hernandez, Y. Itigin, M. Dubman, G. Shainer, R. L. Graham, L. Liss, Y. Shahar, S. Potluri, D. Rossetti, D. Becker, D. Poole, C. Lamb, S. Kumar, C. Stunkel, G. Bosilca, and A. Bouteiller, "Ucx: An open source framework for hpc network apis and beyond," in *2015 IEEE 23rd Annual Symposium on High-Performance Interconnects*, 2015, pp. 40–43.

[44] Y. S. Shao, J. Clemons, R. Venkatesan, B. Zimmer, M. Fojtik, N. Jiang, B. Keller, A. Klinefelter, N. Pinckney, P. Raina, S. G. Tell, Y. Zhang, W. J. Dally, J. Emer, C. T. Gray, B. Khailany, and S. W. Keckler, "Simba: Scaling deep-learning inference with multi-chip-module-based architecture," in *Proceedings of the 52nd Annual IEEE/ACM International Symposium on Microarchitecture*, ser. MICRO '52. New York, NY, USA: Association for Computing Machinery, 2019, p. 144–27. [Online]. Available: <https://doi.org/10.1145/3352460.3358302>

[45] R. Thakur, R. Rabenseifner, and W. Gropp, "Optimization of collective communication operations in mpich," *Int. J. High Perform. Comput. Appl.*, vol. 19, no. 1, pp. 49–66, Feb. 2005. [Online]. Available: <http://dx.doi.org/10.1177/1094342005051521>

[46] K. D. Underwood, J. Coffman, R. Larsen, K. S. Hemmert, B. W. Barrett, R. Brightwell, and M. Levenhagen, "Enabling flexible collective communication offload with triggered operations," in *2011 IEEE 19th Annual Symposium on High Performance Interconnects*, Aug 2011, pp. 35–42.

[47] Y. Wang, Q. Wang, S. Shi, X. He, Z. Tang, K. Zhao, and X. Chu, "Benchmarking the performance and power of ai accelerators for ai training," 2019.

[48] Y. Wu, M. Schuster, Z. Chen, Q. V. Le, M. Norouzi, W. Macherey, M. Krikun, Y. Cao, Q. Gao, K. Macherey, J. Klingner, A. Shah, M. Johnson, X. Liu, L. Kaiser, S. Gouws, Y. Kato, T. Kudo, H. Kazawa, K. Stevens, G. Kurian, N. Patil, W. Wang, C. Young, J. Smith, J. Riesa, A. Rudnick, O. Vinyals, G. Corrado, M. Hughes, and J. Dean, "Google's neural machine translation system: Bridging the gap between human and machine translation," *CoRR*, vol. abs/1609.08144, 2016. [Online]. Available: <http://arxiv.org/abs/1609.08144>